Ultraviolet Light-Based Current–Voltage Method for Simultaneous Extraction of Donor- and Acceptor-Like Interface Traps in β-Ga_2O_3 FETs

Hagyoul Bae, *Member, IEEE*, Jinhyun Noh, Sami Alghamdi, Mengwei Si, and Peide D. Ye, *Fellow, IEEE*

***Abstract*—A novel technique is proposed for the simultaneous extraction of energy distribution of donor- and acceptor-like interface trap states [$D_{it\_D}(E)$ and $D_{it\_A}(E)$] over a wide range of bandgap energy using deep UV light with sub-bandgap ($E_{ph} = h\nu < E_g$) photons less than the bandgap of the β-gallium oxide (β-Ga_2O_3) channel material in the β-Ga_2O_3 field-effect transistors. In the proposed technique, we characterized $D_{it\_D}(E)$ and $D_{it\_A}(E)$ separately based on the difference in the gate voltage (V_{GS})-dependent ideality factors [$d\Delta\eta(V_{GS})/dV_{GS}$] for the photoresponsive carriers excited from D_{it_D}(E) and $D_{it\_A}(E)$ under two different regions ($V_{ON} < V_{GS} < V_{FB}$ and $V_{FB} < V_{GS} < V_T$) in the subthreshold operation.**

***Index Terms*—β-Ga_2O_3 FET, wide bandgap, power device, donor-like trap states, acceptor-like trap states, differential ideality factor, photonic current, sub-threshold current.**

I. Introduction

ULTRA wide bandgap β-Ga_2O_3 FETs are under active development for the next generation power electronics owing to its wide bandgap of 4.8–4.9 eV, high breakdown electric field of 8 MV/cm, as well as its suitability for mass production with low cost fabrication [1]–[8]. Recently, not only optical devices and photo detectors [9]–[11] but also high-power field-effect transistors (FETs) [12], [13] have been reported. Unlike the conventional GaN high-electron mobility transistors (HEMTs) with Schottky gate structures, metal-oxide- semiconductor (MOS)–based devices using a gate insulator effectively achieve more sufficient gate modulation and suppress gate leakage current [14]. Therefore, the interface quality between the gate insulator and the active channel material becomes a critical issue in the characterization of β-Ga_2O_3 FETs for better speed as well as high power applications [15], [16]. Hence, the full experimental characterization of $D_{it}(E)$ over the forbidden bandgap from the valence band maximum (E_V) to the conduction band minimum (E_C) becomes very important in device research. The interface traps, that arise from the interface between the gate oxide and the channel surface could lead to short- or long-term device degradation and impede the high performance and reliability of the devices. Several techniques have been developed to characterize and analyze D_{it} in the MOS system, such as the high/low frequency, photo-assisted current–voltage (I–V), AC conductance, deep–level optical and transient spectroscopy, and Terman method [17]–[22]. In addition, in [19], we analyzed the acceptor-like interface and bulk density-of-states (DOS) using the I-V-based optical charge pumping technique in n-channel amorphous indium-gallium zinc oxide (a-IGZO) thin-film transistors (TFTs). However, the energy range is limited for the DOS close to the E_C, and a general technique for the extraction of DOS close to the E_V is absent. Unlike a-IGZO TFTs, $D_{it}(E)$ is known to be a more critical component than the bulk traps in β-Ga_2O_3 FETs. Therefore, the simultaneous extraction of both $D_{it\_D}(E)$ and $D_{it\_A}(E)$ $eV^{-1}cm^{-2}$ over a wide range of bandgap energies is essential. However, a characterization technique based on only experimental photonic I–V data in β-Ga_2O_3 FETs has never been reported.

In this work, we propose an I–V-based sub-bandgap optoelectronic characterization technique for the simultaneous extraction of $D_{it\_D}(E)$ and $D_{it\_A}(E)$ using deep UV light with sub-bandgap photon energy (E_{ph} = 3.6 eV and λ = 390 nm). By employing the measured I_{DS}–V_{GS} curves under both dark and photonic states, a consistent mapping of the surface potential (ψ_S) for $D_{it\_D}(E)$ and $D_{it\_A}(E)$ over the bandgap energy ($E_C < E < E_V$) was applied in two distinguishable subthreshold regions ($V_{ON} < V_{GS} < V_{FB}$ and $V_{FB} < V_{GS} < V_T$).

II. Device Fabrication

The β-Ga_2O_3 FETs used for our experiments were fabricated with a bottom-gate structure as shown in Fig. 1(a). For the fabrication of the bottom-gate β-Ga_2O_3 FETs, thin (100) β-Ga_2O_3 nano-membranes with Sn doping concentration of 2.7×10^{18} cm^{-3} was transferred from the bulk β-Ga_2O_3 substrate onto the gate oxide (270 nm SiO_2) of a p+ Si wafer, which functioned as a bottom-gate. The SiO_2/Si substrate was cleaned with acetone, methanol, and isopropyl alcohol for 30 min. Afterwards, the source (S) and drain (D) regions were patterned by electron-beam lithography, Ti/Al/Au (15/60/50 nm) metallization, and lift-off process. Fig. 1(b)

Manuscript received September 4, 2018; revised September 18, 2018; accepted September 19, 2018. Date of publication September 24, 2018; date of current version October 23, 2018. This work was supported in part by ASCENT, one of six centers in JUMP, a Semiconductor Research Corporation Program through DARPA, in part by the Office of Naval Research's Naval Enterprise Partnership Teaming with Universities for National Excellence under Grant N00014-15-1-2833, in part by the Defense Threat Reduction Agency under Grant HDTRA1-12-1-0025, and in part by the Basic Science Research Program through the National Research Foundation of Korea through the Ministry of Education under Grant 2018R1A6A3A03013435. The review of this letter was arranged by Editor S. Hall. *(Corresponding author: Peide D. Ye.)*

The authors are with the School of Electrical and Computer Engineering and the Birck Nanotechnology Center, Purdue University, West Lafayette, IN 47907 USA (e-mail: yep@purdue.edu).

Color versions of one or more of the figures in this letter are available online at http://ieeexplore.ieee.org.

Digital Object Identifier 10.1109/LED.2018.2871801

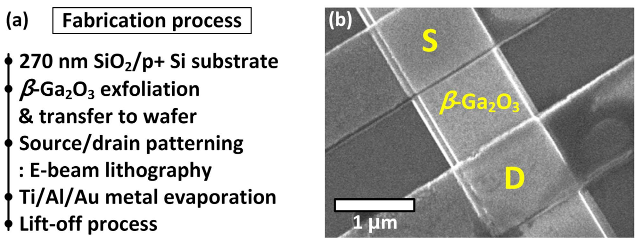

Fig. 1. (a) Process flow for device fabrication of the exfoliated β-Ga_2O_3 nano-membrane FETs with the bottom-gate structure. (b) SEM image of the fabricated device.

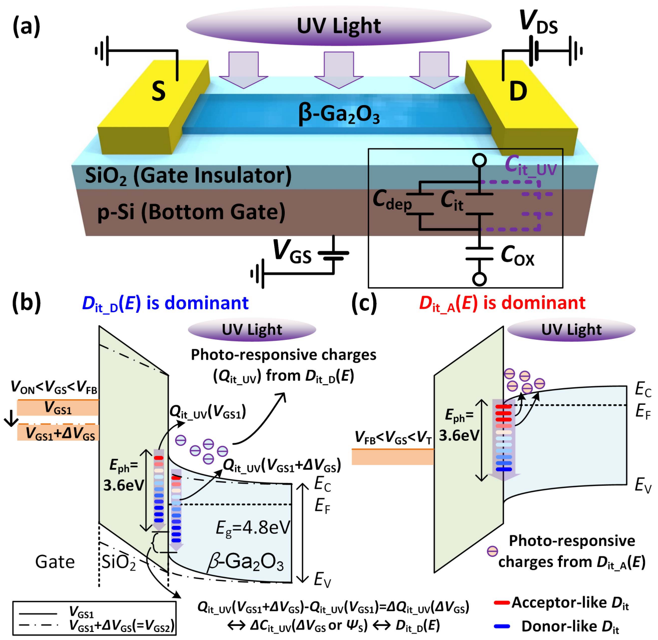

Fig. 2. (a) Schematic view of the measurement setup under a photonic state with the sub-bandgap UV light including the equivalent circuit model as the inset. (b) and (c) Energy band diagrams for the concept of simultaneous extractions of both $D_{it\_D}(E)$ and $D_{it\_A}(E)$.

shows the scanning electron microscope (SEM) image of a fabricated β-Ga_2O_3 FET.

III. Extraction of $D_{it\_D}(E)$ and $D_{it\_A}(E)$ Using Sub-Bandgap UV Light

Fig. 2(a) shows the measurement setup and an equivalent circuit model for the photonic I–V characterization of the β-Ga_2O_3 FETs with bottom-gate structure. A schematic illustration of the energy band diagram for the extraction of $D_{it\_D}(E)$ and $D_{it\_A}(E)$ under a photonic state are shown in Figs. 2(b) and (c). The UV optical source illuminates the β-Ga_2O_3 channel of the fabricated device vertically. UV light ($\lambda = 390$ nm, $E_{ph} = 3.6$ eV $< E_{g\_Ga2O3} = 4.8$ eV, and $P_{opt} = 2.8$ mW) was used to pump the trapped electrons in the channel surface region from E_C–E_{ph} to E_C.

The drain current (I_{D_sub}) in the subthreshold region ($V_{ON} < V_{GS} < V_T$) in the β-Ga_2O_3 FETs can be described as

$$I_{D\_sub} = \mu_{eff} C_{OX} \left(\frac{W}{L}\right) (\eta(V_{GS})-1)\, V_{th}^2 \times \exp\left(\frac{V_{GS}-V_T}{\eta(V_{GS})V_{th}}\right) \tag{1}$$

with $\eta(V_{GS})$ as the ideality factor related to $D_{it}(E)$ controlled by V_{GS}, μ_{eff} as the effective mobility, C_{OX} as the oxide capacitance, W as the channel width, L as the channel length, V_{th} as the thermal voltage. Also, the $\eta(V_{GS})$ can be expressed as

$$\eta(V_{GS}) = \left(\frac{(V_{GS}+\Delta V_{GS})}{V_{th}}\right) \Big/ \ln\left(\frac{I_{D\_sub}(V_{GS}+\Delta V_{GS})}{I_{D\_sub}(V_{GS})}\right) \tag{2}$$

with ΔV_{GS} as step of V_{GS} [13]. For the $\eta(V_{GS})$ under dark and photonic states, each component is also described as

$$\eta_{dark}(V_{GS}) = 1 + \left(C_{dep}(V_{GS}) + C_{it}(V_{GS})\right)/C_{OX} \tag{3}$$

$$\eta_{UV}(V_{GS}) = 1 + \left(C_{dep}(V_{GS}) + C_{it}(V_{GS}) + C_{it\_UV}(V_{GS})\right)/C_{OX} \tag{4}$$

with $C_{it}(V_{GS})$ as the interface traps-induced capacitance under dark state, $C_{it\_UV}(V_{GS})$ as the photo-responsive capacitance for the photo-excited charges, and $C_{dep}(V_{GS})$ as the depletion capacitance. In eq. (4), the $\eta_{UV}(V_{GS})$ includes photo-responsive charges generated from $D_{it\_D}(E)$ and $D_{it\_A}(E)$ by sub-bandgap photon as shown in Fig. 2. The $\Delta\eta(V_{GS})$ as the difference between $\eta_{dark}(V_{GS})$ and $\eta_{UV}(V_{GS})$ can be expressed as

$$\Delta\eta(V_{GS}) = \eta_{UV}(V_{GS}) - \eta_{dark}(V_{GS}) = C_{it\_UV}(V_{GS})/C_{OX}. \tag{5}$$

We can determine the $\Delta C_{it\_UV}(V_{GS})$ through eqs. (6) $\sim$ (8)

$$C_{it\_UV}(V_{GS}) = C_{OX}\Delta\eta(V_{GS}) \tag{6}$$

$$d\Delta\eta(V_{GS})/dV_{GS} = \left((dC_{it\_UV}(V_{GS})/d\psi_S)\cdot(d\psi_S/dV_{GS})\right)/C_{OX} \tag{7}$$

$$\Delta C_{it\_UV}(V_{GS}) = C_{OX}\int_{\psi_S(V_{GS})}^{\psi_S(V_{GS}+\Delta V_{GS})}\left(\frac{d\Delta\eta(V_{GS})}{dV_{GS}}\Big/\frac{d\psi_S}{dV_{GS}}\right) \times d\psi_S. \tag{8}$$

In the extraction of $D_{it\_D}(E)$ and $D_{it\_A}(E)$ as illustrated in Fig. 2(b) and (c), eq. (8) can be converted to $\Delta C_{it\_D}(V_{GS})$ and $\Delta C_{it\_A}(V_{GS})$ over two different regions ($V_{ON} < V_{GS} < V_{FB}$ and $V_{FB} < V_{GS} < V_T$) with ΔV_{GS} as follow respectively:

$$\Delta C_{it\_D}(V_{GS}) = C_{OX}\int_{\psi_S(V_{ON})}^{\psi_S(V_{FB})}\left(\frac{d\Delta\eta_D(V_{GS})}{dV_{GS}}\Big/\frac{d\psi_S}{dV_{GS}}\right)d\psi_S \tag{9}$$

$$\Delta C_{it\_A}(V_{GS}) = C_{OX}\int_{\psi_S(V_{FB})}^{\psi_S(V_T)}\left(\frac{d\Delta\eta_A(V_{GS})}{dV_{GS}}\Big/\frac{d\psi_S}{dV_{GS}}\right)d\psi_S. \tag{10}$$

For the mapping of the V_{GS} to the specific trap energy level for both $D_{it\_D}(E)$ and $D_{it\_A}(E)$ over the bandgap, the measured $I_{D\_sub}(V_{GS})$ was also divided into two operation regions ($V_{ON} < V_{GS} < V_{FB}$ and $V_{FB} < V_{GS} < V_T$). Then, the $\psi_S(V_{GS})$ corresponding to V_{GS} was calculated as [19].

Finally, $D_{it\_D}(E)$ and $D_{it\_A}(E)$ can be extracted through

$$D_{it\_D}(E) = \Delta C_{it\_D}(V_{GS})/q^2 \quad \text{and} \quad D_{it\_A}(E) = \Delta C_{it\_A}(V_{GS})/q^2. \tag{11}$$

IV. Experimental Results and Discussions

To extract $D_{it\_D}(E)$ and $D_{it\_A}(E)$ by the photonic I–V technique, we measured the I_{DS}–V_{GS} and I_{G-R} characteristics (Keysight B1500 Semiconductor Parameter Analyzer and a Cascade Summit probe station) of the β-Ga_2O_3 FETs with bottom-gate structure. The representative β-Ga_2O_3 FET has a channel length of $L = 1$ μm and a channel width

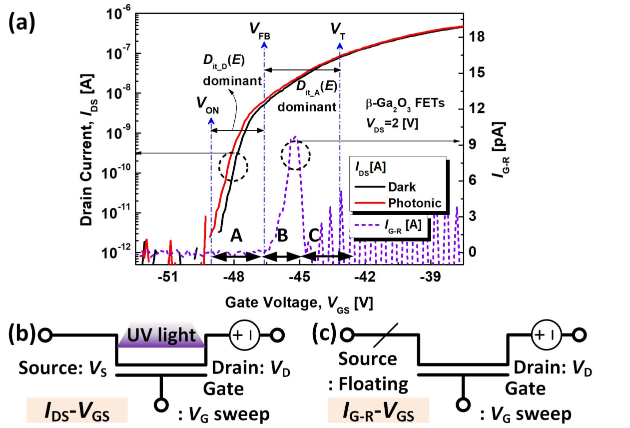

Fig. 3. (a) Measured I_{DS}-V_{GS} characteristics under dark (black line) and photonic (red line) states. The I_{G-R} (dash line) was measured with the source terminal floating. Measurement setup for (b) I_{DS}-V_{GS} with UV light and (c) I_{G-R}.

of $W = 1\ \mu$m. Fig. 3 shows the measured I_{DS}–V_{GS} characteristics under both dark and photonic states and the I_{G-R}–V_{GS} curve. Threshold voltage (V_T) was defined by the linear extrapolation method and flatband voltage (V_{FB}) was extracted at the point where the I_{G-R} increases. A negligible hysteresis occurs for the measured I_D–V_{GS} characteristics without any passivation and post–annealing process [23]. It is well known that the electrons arising from $D_{it}(E)$ according to the ΔV_{GS} correspond to those from a specific ψ_S or energy level over the bandgap. To minimize the errors caused by the incident sub-bandgap photons (E_{ph} (= 3.6 eV) < E_g (= 4.8 eV)), we applied the optically excited charges ($\Delta C_{it\_UV} \leftrightarrow \Delta Q_{it\_UV}$) by taking a differentiation by V_{GS}, as shown in eq. (8). However, more advanced analysis is needed to avoid the potential underestimation of $D_{it}(E)$, because both photoexcited electrons from the trap states to the E_C and those from the E_V to the trap states can affect the photonic I-V characterization. To fully pump out the carriers from $D_{it\_D}(E)$ and $D_{it\_A}(E)$, which are located in the range from E_C to E_V, UV light with E_{ph} = 3.6 eV was used. Further, the measured I_{G-R} as a function of V_G at $V_D = 2$ V is shown in Fig. 3(a). Initially, the I_{G-R} is negligible because the energy difference between the Fermi energy E_F and E_C near the channel interface is large compared with the thermal energy when V_G is less than V_{FB}. Additionally, the amount of thermally generated charges that can contribute to the I_{G-R} is insufficient because the source terminal is floating (A region in Fig. 3(a)). As V_G increases, the I_{G-R} at the drain side increases by the thermal generation because E_F becomes closer to E_C in the channel region near the interface (B region in Fig. 3(a)). Meanwhile, I_{G-R} decreases when V_G is larger than the V_{FB} because the recombination process in C region is relatively increase as compared with that in B region as both the electron concentration and empty interface trap states increase (C region in Fig. 3(a)). The measurement setups for the I_{DS}–V_{GS} curves under a photonic state with UV light and I_{G-R}–V_{GS} characteristic are shown in the Figs. 3(b) and (c), respectively. Accordingly, the I_{G-R} data was utilized to determine the V_{FB} and distinguish between $D_{it\_D}(E)$ and $D_{it\_A}(E)$ [24]. In the depletion region ($V_{ON} < V_{GS} < V_{FB}$), the photo-responsive charges generated from $D_{it\_D}(E)$ primarily affect I_{DS}, while the photo-responsive charges excited from $D_{it\_A}(E)$ contribute to the I_{DS} in the accumulation region ($V_{FB} < V_{GS} < V_T$).

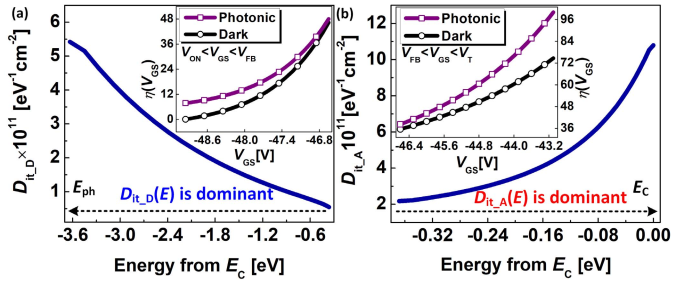

Fig. 4. Energy distribution of extracted D_{it} [(a): $D_{it\_D}(E)$ and (b): $D_{it\_A}(E)$] via photo-responsive I-V characteristics with sub-bandgap UV light. The inset shows the extracted $\eta(V_{GS})$.

Fig. 4 shows the $D_{it\_D}(E)$ and $D_{it\_A}(E)$ obtained from the proposed photonic I–V technique. The V_{GS}-dependent experimental $\eta_{dark}(V_{GS})$ and $\eta_{UV}(V_{GS})$ in two distinguishable regions ($V_{ON} < V_{GS} < V_{FB}$ and $V_{FB} < V_{GS} < V_T$) are shown in the insets of Figs. 4(a) and (b), respectively. Through the proposed technique, we obtained D_{it_D}(E) and $D_{it\_A}(E)$ over the subgap energy ranges of 0.5×10^{11} eV^{-1}cm^{-2} to 5.5×10^{11} eV^{-1}cm^{-2} and of 2.1×10^{11} eV^{-1}cm^{-2} to 1.1×10^{12} eV^{-1}cm^{-2}, respectively. The extracted values obtained in this work are comparable to those of other reports [15], [16].

It is worth noting that this proposed technique allows the simultaneous characterization of $D_{it\_D}(E)$ and $D_{it\_A}(E)$ with a wide range of bandgap energies by applying the calculated ψ_S separately in two distinguishable subthreshold regions, instead of a single ψ_S over the full subthreshold range. We also found that the C–V-based extraction method, which requires large-sized devices, has a limit on the parasitic component correction for the accurate extraction of $D_{it}(E)$ in the β-Ga_2O_3 channel region only, excluding the contribution from the gate-to-source and gate-to-drain overlapped regions. Meanwhile, this technique has a limit when it is applied to top-gate devices because the incident light cannot pass through the gate metal. In this regard, two possible methods can be used to improve the applicability of this technique: 1) irradiation of the tilted light on the top of the device, and 2) irradiation of the backlight at the bottom of the device with a transparent substrate. In addition, further experiments for photonic I–V characterization with various β-Ga_2O_3 thicknesses are required to confirm the effect of both the interface and bulk traps because possible errors still remain in the extracted $D_{it\_D}(E)$ and $D_{it\_A}(E)$ owing to the overestimated charges from the bulk traps of the β-Ga_2O_3 film by incident light. Therefore, we expect that a comprehensive technique using an optical source is required for the characterization of trap density considering the device geometry, as a further study.

V. Conclusion

In this work, a sub-bandgap UV light-based photonic I–V technique based on a differential subthreshold ideality factor in the dark and photonic states was proposed for the extraction of $D_{it}(E)$ over a wide range of bandgap energies in β-Ga_2O_3 FETs. We found that the extracted $D_{it}(E)$ is fully separated into $D_{it\_D}(E)$ and $D_{it\_A}(E)$ based on the photo-responsive carriers generated by the sub-bandgap UV light and the I_{G-R} configuration for the generation and recombination processes. This proposed method has the advantage of simplicity compared to other techniques.

References

[1] M. Higashiwaki, K. Sasaki, A. Kuramata, T. Masui, and S. Yamakoshi, "Gallium oxide (Ga_2O_3) metal-semiconductor field-effect transistors on single-crystal β-Ga_2O_3 (010) substrates," *Appl. Phys. Lett.*, vol. 100, no. 1, p. 013504, Jan. 2012, doi: 10.1063/1.3674287.

[2] K. Sasaki, M. Higashiwaki, A. Kuramata, T. Masui, and S. Yamakoshi, "MBE grown Ga_2O_3 and its power device applications," *J. Cryst. Growth*, vol. 378, pp. 591–595, Sep. 2013, doi: 10.1016/.j.jcrysgro.2013.02.015.

[3] S. Rafique, L. Han, A. T. Neal, S. Mou, M. J. Tadjer, R. H. French, and H. Zhao, "Heteroepitaxy of N-type β-Ga_2O_3 thin films on sapphire substrate by low pressure chemical vapor deposition," *Appl. Phys. Lett.*, vol. 109, no. 13, p. 132103, Sep. 2016, doi: 10.1063/1.4963820.

[4] S. Rafique, L. Han, M. J. Tadjer, J. A. Freitas, Jr., N. A. Mahadik, and H. Zhao, "Homoepitaxial growth of β-Ga_2O_3 thin films by low pressure chemical vapor deposition," *Appl. Phys. Lett.*, vol. 108, no. 18, p. 182105, May 2016, doi: 10.1063/1.4948944.

[5] S. W. Kaun, F. Wu, and J. S. Speck, "β-$(Al_xGa_{1-x})_2O_3/Ga_2O_3$ (010) heterostructures grown on β-Ga_2O_3 (010) substrates by plasma-assisted molecular beam epitaxy," *J. Vac. Sci. Technol. A, Vac., Surfaces, Films*, vol. 33, no. 4, p. 041508, Jun. 2015, doi: 10.1116/1.4922340.

[6] N. Ueda, H. Hosono, R. Waseda, and H. Kawazoe, "Synthesis and control of conductivity of ultraviolet transmitting β-Ga_2O_3 single crystals," *Appl. Phys. Lett.*, vol. 70, no. 26, p. 3561, Nov. 1998, doi: 10.1063/1.119233.

[7] Y. Tomm, P. Reiche, D. Klimm, and T. Fukuda, "Czochralski grown Ga_2O_3 crystals," *J. Cryst. Growth*, vol. 220, no. 4, pp. 510–514, Dec. 2000, doi: 10.1016/S0022-0248(00)00851-4.

[8] H. Aida, K. Nishiguchi, H. Takeda, N. Aota, K. Sunakawa, and Y. Yaguchi, "Growth of β-Ga_2O_3 single crystals by the edge-defined, film fed growth method," *Jpn. J. Appl. Phys.*, vol. 47, no. 11R, pp. 8506–8509, Nov. 2008, doi: 10.1143/JJAP.47.8506.

[9] S. Nakagomi, T. Momo, S. Takahashi, and Y. Kokubun, "Deep ultraviolet photodiodes based on β-Ga_2O_3/SiC heterojunction," *Appl. Phys. Lett.*, vol. 103, no. 7, p. 072105, Aug. 2013, doi: 10.1063/1.4818620.

[10] Y. Kokubun, K. Miura, F. Endo, and S. Nakagomi, "Sol-gel prepared β-Ga_2O_3 thin films for ultraviolet photodetectors," *Appl. Phys. Lett.*, vol. 90, no. 3, p. 031912, Jan. 2007, doi: 10.1063/1.2432946.

[11] T. Oshima, T. Okuno, N. Arai, N. Suzuki, S. Ohira, and S. Fujita, "Vertical solar-blind deep-ultraviolet Schottky photodetectors based on β-Ga_2O_3 substrates," *Appl. Phys. Exp.*, vol. 1, no. 1, pp. 011202-1–011202-3, Jan. 2008, doi: 10.1143/APEX.1.011202.

[12] A. J. Green, K. D. Chabak, E. R. Heller, R. C. Fitch, M. Baldini, A. Fiedler, K. Irmscher, G. Wagner, Z. Galazka, S. E. Tetlak, A. Crespo, K. Leedy, and G. H. Jessen, "3.8-MV/cm breakdown strength of MOVPE-grown Sn-doped β-Ga_2O_3 MOSFETs," *IEEE Electron Device Lett.*, vol. 37, no. 7, pp. 902–905, Jul. 2016, doi: 10.1109/LED.2016.2568139.

[13] W. S. Hwang, A. Verma, H. Peelaers, V. Protasenko, S. Rouvimov, H. Xing, A. Seabaugh, W. Haensch, C. van de Walle, Z. Galazka, M. Albrecht, R. Fornari, and D. Jena, "High-voltage field effect transistors with wide-bandgap β-Ga_2O_3 nanomembranes," *Appl. Phys. Lett.*, vol. 104, no. 20, p. 203111, May 2014, doi: 10.1063/1.4879800.

[14] M. A. Khan, X. Hu, G. Sumin, A. Lunev, J. Yang, R. Gaska, and M. S. Shur, "AlGaN/GaN metal oxide semiconductor heterostructure field effect transistor," *IEEE Electron Device Lett.*, vol. 21, no. 2, pp. 63–65, Feb. 2000, doi: 10.1109/55.821668.

[15] H. Zhou, S. Alghmadi, M. Si, G. Qiu, and P. D. Ye, "Al_2O_3/β-Ga_2O_3(-201) interface improvement through piranha pretreatment and postdeposition annealing," *IEEE Electron Device Lett.*, vol. 37, no. 11, pp. 1411–1414, Nov. 2016, doi: 10.1109./LED.2016.2609202.

[16] K. Zeng, Y. Jia, and U. Singisetti, "Interface state density in atomic layer deposited SiO_2/β-$Ga_2O_3(\bar{2}01)$ MOSCAPs," *IEEE Electron Device Lett.*, vol. 37, no. 7, pp. 906–909, Jul. 2016, doi: 10.1109./LED.2016.2570521.

[17] E. H. Nicollian and J. R. Brews, *MOS (Metal Oxide Semiconductor) Physics and Technology*. Hoboken, NJ, USA: Wiley, 1982.

[18] D. K. Schroder, *Semiconductor Material and Device Characterization*, 3rd ed. New York, NY, USA: Wiley, 2006, pp. 319–374.

[19] H. Bae, H. Seo, S. Jun, H. Choi, J. Ahn, J. Hwang, J. Lee, S. Oh, J.-U. Bae, S.-J. Choi, D. H. Kim, and D. M. Kim, "Fully current-based sub-bandgap optoelectronic differential ideality factor technique and extraction of subgap DOS in amorphous semiconductor TFTs," *IEEE Trans. Electron Devices*, vol. 61, no. 10, pp. 3566–3569, Oct. 2014, 10.1109/TED.2014.2348592.

[20] L. M. Terman, "An investigation of surface states at a silicon/silicon oxide interface employing metal-oxide-silicon diodes," *Solid-State Electron.*, vol. 5, no. 5, pp. 285–299, Sep./Oct. 1962, doi: 10.1016/0038-1101(62)90111-9.

[21] Z. Zhang, E. Farzana, A. R. Arehart, and S. A. Ringel, "Deep level defects throughout the bandgap of (010) β-Ga_2O_3 detected by optically and thermally stimulated defect spectroscopy," *Appl. Phys. Lett.*, vol. 108, no. 5, p. 052105, Feb. 2016, doi: 10.1063/1.4941429.

[22] Y. Nakano, "Communication—Electrical characterization of β-Ga_2O_3 single crystal substrates," *ECS J. Solid State Sci. Technol.*, vol. 6, no. 9, pp. P615–P617, Aug. 2017, doi: 10.1149/2.0181709jss.

[23] H. Zhou, M. Si, S. Alghamdi, G. Qiu, L. Yang, and P. D. Ye, "High-performance depletion/enhancement-ode β-Ga_2O_3 on insulator (GOOI) field-effect transistors with record drain currents of 600/450 mA/mm," *IEEE Electron Device Lett.*, vol. 38, no. 1, pp. 103–106, Jan. 2017, doi: 10.1109/LED.2016.2635579.

[24] S. M. Sze and K. K. Ng, *Physics Of Semiconductor Devices*, 3rd ed. New York, NY, USA: Wiley, 2007, pp. 40–45.